arXiv:1402.0959v1 [astro-ph.HE] 5 Feb 2014

Neutrino Emissivities from Deuteron-Breakup and Formation in Supernovae

S. Nasu

Department of Physics, Osaka University, Toyonaka, Osaka 560-0043, Japan

nasu@phys.sci.osaka-u.ac.jp

S. X. Nakamura

Department of Physics, Osaka University, Toyonaka, Osaka 560-0043, Japan

nakamura@kern.phys.sci.osaka-u.ac.jp

K. Sumiyoshi

Numazu College of Technology, Ooka 3600, Numazu, Shizuoka 410-8501, Japan

sumi@numazu-ct.ac.jp

T. Sato

Department of Physics, Osaka University, Toyonaka, Osaka 560-0043, Japan

tsato@phys.sci.osaka-u.ac.jp

F. Myhrer

Department of Physics and Astronomy, University of South Carolina, Columbia SC 29208, USA

myhrer@physics.sc.edu

and

K. Kubodera

Department of Physics and Astronomy, University of South Carolina, Columbia SC 29208, USA

kubodera@caprine.physics.sc.edu

Received _____; accepted _____

Prepared for submission to Astrophys. J.

ABSTRACT

Neutrino emissions from electron/positron capture on the deuteron and the nucleon-nucleon fusion processes in the surface region of a supernova core are studied. These weak processes are evaluated in the standard nuclear physics approach, which consists of one-nucleon and two-nucleon-exchange currents and nuclear wave functions generated by a high precision nucleon-nucleon potential. In addition to the cross sections for these processes involving the deuteron, we present neutrino emissivities due to these processes calculated for typical profiles of core-collapsed supernovae. These novel neutrino emissivities are compared with the standard neutrino emission mechanisms. We find that the neutrino emissivity due to the electron capture on the deuteron is comparable to that on the proton in the deuteron abundant region. The implications of the new channels involving deuterons for the supernova mechanism are discussed.

Subject headings: Neutrino emissivity,deuteron formation, supernova

1. Introduction

The neutrinos play pivotal roles in core-collapse supernovae and their subsequent evolution to neutron stars. Neutrino reactions in the dense matter of a supernova core are crucial for understanding the supernova explosion mechanism, which is still elusive despite extensive studies over decades. It is therefore essential to identify all neutrino processes, both neutrino-emission and neutrino-absorption processes, that can be important in the supernova environment. Failing to include all the relevant neutrino processes in supernova modeling may have significant consequences for the theoretical understanding of the supernova explosion. The emission of neutrinos acts as a cooling mechanism of the central core, and the addition of any neutrino emission channels that have not been considered so far could affect this cooling mechanism. A portion of the emitted neutrinos are subsequently absorbed by the material behind the shock wave and thereby act as a heating agent. Additional sources of neutrinos enhance this neutrino-heating mechanism and may help the revival of the stalled shock wave and lead to a successful modeling of supernova explosion (Bethe 1990; Kotake et al. 2006; Janka et al. 2007). The neutrinos emitted gradually ($\sim$20 s) from a nascent neutron star (proto-neutron star) in a supernova explosion, can be detected as supernova neutrinos at terrestrial neutrino detectors, like in the case of SN1987A (Suzuki 1994), and can be a useful source of information about the neutrino emission mechanisms.

Recent calculations have shown that deuterons, tritons and ^{3}He can appear copiously in the regions between the supernova core and the shockwave (Sumiyoshi & Röpke 2008; Arcones et al. 2008; Hempel et al. 2012). These light elements have so far not been included in the tables of equation of state (EOS) (Lattimer & Swesty 1991; Shen et al. 1998a,b) that are routinely used in supernova simulations where the nuclear species are limited to the proton, neutron, ^{4}He and one "representative heavy nucleus" that is assumed to

simulate the roles of all heavy nuclei. The light elements with mass number $A = 2$ and 3 can be abundant in hot and moderately dense matter ($< 10^{13} g/cm^3$) under nuclear statistical equilibrium (Sumiyoshi & Röpke 2008; Arcones et al. 2008; Hempel et al. 2012; Furusawa et al. 2013b) and should be considered in studying the supernova mechanism. They appear in the heating region behind a shockwave, and also in the cooling region at the surface of a proto-neutron star; their appearance gives a new contribution to the neutrino opacity. For example, Sumiyoshi & Röpke (2008) showed in a snapshot 150 msec after the bounce that the deuteron mass fraction amounts to about 10% in the neutrino-emitting cooling regions at densities $\sim 10^{11}$-10^{12} g/cm^3. Neutrino processes in this cooling region are essential for determining the flux and spectra of emitted neutrinos, which in turn affect the efficiency of neutrino heating behind the shockwave. Nakamura et al. (Nakamura et al. 2009) investigated neutrino absorption on deuterons as an additional heating mechanism on top of the neutrino reactions on nucleons and ^{4}He, while Arcones et al. (Arcones et al. 2008) studied neutrino reactions on tritons and ^{3}He to evaluate their influences on the neutrino spectra at the outer layer of a proto-neutron star.

According to Refs. Sumiyoshi & Röpke (2008); Arcones et al. (2008), the deuteron fraction can be larger than the proton fraction in part of the neutrino-sphere region between the shock wave and the proto-neutron star surface. This indicates that weak-interaction deuteron breakup may play a significant role in neutrino emission processes, possibly altering the conventional understanding of the role of the protons in the neutrino-emission processes as well as the neutronization of matter. An additional reaction to be investigated in this work is deuteron formation in nucleon-nucleon scattering, which also leads to neutrino emission. Although both these neutrino emission processes certainly exist on top of the conventional neutrino-emission processes, they have so far not been considered in supernova simulations.

In this article we study neutrino emissions from deuteron breakup/formation processes (DBF for short) in the surface region of a proto-neutron star, where neutrino emissions act as a cooling mechanism. We present the first evaluation of the neutrino emissivities from electron/position-capture on the deuteron (deuteron breakup) and from the nucleon-nucleon weak fusion processes (deuteron formation); see (1)-(5) below. The neutrino emissivities arising from DBF will be compared with those coming from the "conventional" processes; by "conventional" processes we mean the neutrino emission processes which have been previously considered in the literature, and which are listed in (6)-(11) below. The neutrino emissivities due to DBF reported here are expected to be useful for numerical simulations of supernova explosion and proto-neutron star cooling.

Theoretical treatments of electroweak processes in two-nucleon systems are well developed. For low-energy neutrino-deuteron reactions, serious efforts to reduce theoretical uncertainties have been made in order to analyze data from the Sudbury Neutrino Observatory (Nakamura et al. 2001, 2002). One approach is the standard nuclear physics approach (SNPA) that involves nuclear wave functions derived from high-precision phenomenological nuclear potentials, and one-nucleon and two-nucleon electroweak currents. SNPA has been well tested by analyses of photo-reactions, electron scattering, and muon capture on the two-nucleon systems (Doi et al. 1990; Tamura et al. 1992; Sato et al. 1995). Another theoretical approach, effective field theory (EFT) consisting of nucleons and pions, has been developed and applied to low-energy electroweak processes (Kubodera & Park 2004). Both methods essentially agree with each other for low-energy electroweak processes in the two-nucleon systems. The pp-fusion process, $pp \to de^+\nu_e$, is one of such processes relevant to this work. This reaction has been studied with both SNPA and EFT, and good agreement between the two methods has been found (Schiavilla et al. 1998; Park et al. 2003). Another nucleon-nucleon fusion process relevant to this work is neutron-neutron fusion, which was previously studied with EFT (Ando & Kubodera 2006). In the present

work we adopt SNPA.

This article is arranged as follows. In section 2 we discuss neutrino emissions via DBF relevant to the supernova environment. The theoretical framework for calculating the cross sections for neutrino emission via DBF and the corresponding neutrino emissivities are outlined in section 3, and the numerical results are presented in sections 4 and 5. The implications and a summary of these results for the supernova mechanism are discussed in section 6.

2. Neutrino Reactions Involving the Deuteron

We consider neutrino emissions via deuteron breakup/formation (DBF):

$$d + e^- \rightarrow n + n + \nu_e \ , \tag{1}$$

$$d + e^+ \rightarrow p + p + \bar{\nu}_e \ , \tag{2}$$

$$n + n \rightarrow d + e^- + \bar{\nu}_e \ , \tag{3}$$

$$p + p \rightarrow d + e^+ + \nu_e \ , \tag{4}$$

$$p + n \rightarrow d + \nu + \bar{\nu} \ . \tag{5}$$

The reactions (1) and (2) are deuteron breakup via e^-/e^+-capture, whereas the reactions (3), (4) and (5) are deuteron formation through nucleon-nucleon scattering. The first four reactions that are caused by the charged-current (CC), can only emit ν_e or $\bar{\nu}_e$, whereas the last reaction occurring via the neutral-current (NC) gives rise to $\nu\bar{\nu}$ pair-emission of all three flavors.

The reactions (1)-(5) are to be compared with the conventional neutrino-emission reactions that have been routinely included in the study of supernovae and neutron stars.

They are:

$$p + e^- \rightarrow n + \nu_e \ , \tag{6}$$

$$n + e^+ \rightarrow p + \bar{\nu}_e \ , \tag{7}$$

$$n + n \rightarrow p + n + e^- + \bar{\nu}_e \ , \tag{8}$$

$$p + p \rightarrow p + n + e^+ + \nu_e \ , \tag{9}$$

$$N + N' \rightarrow N + N' + \nu + \bar{\nu} \ , \tag{10}$$

$$e^- + e^+ \rightarrow \nu + \bar{\nu} \ . \tag{11}$$

Reactions (6) and (7) represent the direct Urca processes, in which e^-/e^+-captures on a single nucleon produce $\nu_e/\bar{\nu}_e$. Reactions (8) and (9) are the modified Urca processes, where nucleon-nucleon collisions lead to $\bar{\nu}_e/\nu_e$ emission. In the last two reactions a pair of $\nu\bar{\nu}$ of all flavors is produced; it is a common practice to refer to the process (10) as nucleon-nucleon bremsstrahlung and the process (11) as e^+e^- annihilation.

The NC reactions produce pairs of $\nu\bar{\nu}$ and act as a cooling mechanism. When the CC reactions take place frequently enough, the proton and neutron fractions are determined through β-equilibrium, $\mu_e = \mu_n - \mu_p + \mu_\nu$. Inside the proto-neutron star, chemical equilibrium is realized among electrons, positrons, nucleons and neutrinos. At the surface of the proto-neutron star(densities $\sim 10^{11} - 10^{13}\mathrm{g/cm}^3$) where neutrinos are not trapped, one must solve the neutrino transfer equation with detailed information about the neutrino reaction rates, in order to determine the neutrino distribution and its evolution associated with the change of matter composition. We note that the reaction rates depend on the degeneracy of leptons and nucleons in the supernova environment; the high degeneracy of the leptons and/or nucleons can significantly suppress the reaction rates. This makes it important to take a proper account of the Pauli blocking factors for particles participating in the reactions.

2.1. Deuteron Breakup via Electron/Positron Capture

The e^-/e^+-capture reactions on the deuteron, (1) and (2), may influence significantly the $\nu_e/\bar{\nu}_e$ emissivities *at the surface* of a proto-neutron star, where deuterons could be abundant (Sumiyoshi & Röpke 2008; Arcones et al. 2008). In a supernova simulation that includes the deuteron abundance (or, more generally, the light element abundance), there are fewer free nucleons and more bound nucleons than in conventional supernova simulations. Therefore, depending on whether the e^-/e^+-capture rates on the deuteron are larger or smaller than those on the proton, the net capture rate per proton (both free and bound protons counted) is enhanced or suppressed by the deuteron abundance. As will be presented, we find the latter to be the case.

Just like the first direct Urca process (6), e^--capture on the deuteron acts as a source of neutronization of the proto-neutron star and drives the dense matter toward the neutron-rich side by changing protons into neutrons with neutrino emissions. Similar to the second direct Urca process (7), e^+-capture on the deuteron acts as a counter reaction, changing neutrons into protons. In addition, in matter with trapped neutrinos (density $> 10^{12}\mathrm{g/cm^3}$) the reversed reactions (neutrino absorptions) may take place as well. The balance between neutrons and protons are determined through quasi-equilibrium and the speed of deleptonization by neutrino emissions.

2.2. Deuteron Formation from Nucleon-Nucleon Scattering

The deuteron formation processes from two nucleons, (3), (4) and (5), take place regardless of the abundance of deuterons. The CC processes, (3) and (4), occur in addition to the modified Urca processes, (8) and (9), and the direct Urca processes (6) and (7). They are part of the reactions which determine the matter composition under quasi-chemical

equilibrium. As is well known, in cold neutron stars when the proton fraction is small enough, the direct Urca process (6) is hindered, and the modified Urca process (8) is essential for cooling. The processes with positrons in the initial state are hindered in cold neutron stars, where electrons are degenerate and positrons are scarce. In a non-degenerate situation where the temperature is high enough, both the processes, (3) and (4), can proceed in the supernova core environment.

The process (5) is a new NC process to be considered in addition to conventional nucleon-nucleon bremsstrahlung, (10). Nucleon-nucleon bremsstrahlung with $\nu\bar{\nu}$ pair emission is one of the main cooling mechanisms of cold neutron stars. Suzuki (Suzuki 1993) pointed out the importance of this process as a dominant source of $\nu_\mu/\bar{\nu}_\mu$ and $\nu_\tau/\bar{\nu}_\tau$ pair-creation in proto-neutron star cooling; it is to be noted that $\nu_\mu/\bar{\nu}_\mu$ and $\nu_\tau/\bar{\nu}_\tau$ carry away energy with almost no energy deposition in the heating region(Bethe 1990; Kotake et al. 2006; Janka et al. 2007). We show in the next sections that the additional $\nu\bar{\nu}$ producing channel, $NN \to d\nu\bar{\nu}$, can be important for the cooling of a proto-neutron star.

3. Calculation of cross sections and neutrino emissivities

The Hamiltonian for low-energy semi-leptonic weak processes is, to good accuracy, given by the product of the hadron current (J^λ) and the lepton current (L^λ) as

$$H_W^{CC} = \frac{G'_F V_{ud}}{\sqrt{2}} \int d\vec{x}[J_\lambda^{CC}(\vec{x}) L_{CC}^\lambda(\vec{x}) + \text{h. c.}] \ , \tag{12}$$

$$H_W^{NC} = \frac{G'_F}{\sqrt{2}} \int d\vec{x}[J_\lambda^{NC}(\vec{x}) L_{NC}^\lambda(\vec{x}) + \text{h. c.}] \ , \tag{13}$$

for the CC and NC processes, respectively. The weak coupling constant $G'_F = 1.1803 \times 10^{-5}$ GeV^{-2} is taken from Nakamura et al. (2002), and the CKM matrix element $V_{ud} = 0.9740$ is given in Beringer et al. (2012). The hadronic weak currents are combinations of the vector

current V^λ and the axial-vector current A^λ:

$$J_\lambda^{CC} = V_\lambda^\pm - A_\lambda^\pm \ , \tag{14}$$

$$J_\lambda^{NC} = (1 - 2\sin^2\theta_W)V_\lambda^3 - A_\lambda^3 - 2\sin^2\theta_W V_\lambda^s \ . \tag{15}$$

In the charged current J_λ^{CC}, the superscript $+(-)$ denotes the isospin raising (lowering) operator. In the neutral current J_λ^{NC}, the superscript '3' denotes the third component of the isovector current, while V_λ^s is the iso-scalar vector current, and θ_W is the Weinberg angle. The corresponding lepton currents are given by

$$\begin{aligned} L_\lambda^{CC} &= \bar{\psi}_l\gamma_\lambda(1-\gamma_5)\psi_\nu \quad \text{for CC reactions} \\ L_\lambda^{NC} &= \bar{\psi}_\nu\gamma_\lambda(1-\gamma_5)\psi_\nu \quad \text{for NC reactions} \end{aligned} \tag{16}$$

The nuclear weak currents consist of one-nucleon [impulse-approximation (IA)] terms and two-nucleon meson-exchange current (MEC) terms. In this work we consider the pion and rho meson-exchange currents. The validity of this approach has been well tested for the vector current by comparing the model predictions with, e.g., the measured $n + p \to d + \gamma$ reaction data. As for the strength of the axial-vector exchange current, we follow the standard practice to adjust its strength to reproduce the experimental triton beta decay rate (Schiavilla et al. 1998). Detailed descriptions of the model for the nuclear currents used in the present work are given in Nakamura et al. (2001, 2002), where the basic formulation and relevant input parameters are explained.

In this article we evaluate the cross sections and emissivities for the DBF processes, (1) - (5). The cross section is given in the standard way as

$$\sigma^\alpha_{i\to f} = \frac{(2\pi)^4}{s_f v_{rel}} \int \prod_l \frac{d\vec{p}_{f,l}}{(2\pi)^3}\delta^{(4)}(\sum_{l'} p_{f,l'} - \sum_{k'} p_{i,k'}) \prod_{k''} \frac{1}{2s_{i,k''}+1} \sum_{i,f} | < f|H^\alpha_W|i > |^2, \tag{17}$$

where v_{rel} and s_f are the relative velocity of the incoming particles and the symmetry factor for the identical two nucleons in the final(initial) state. The summation $\sum_{i,f}$ over the spin

states of the final particles and the average over the initial spin states with spin $s_{i,k''}$. The momenta of the initial (final) particles, labeled by k (l), are $\vec{p}_{i,k}$ ($\vec{p}_{f,l}$).

The emissivities for neutrinos and anti-neutrino are denoted by Q_ν and $Q_{\bar{\nu}}$, respectively. They are given by integrating the transition probability over the momenta $\vec{p}_{i,k}$ and $\vec{p}_{f,l}$ with a weighting factor representing the momentum distributions:

$$\begin{aligned} Q^{\alpha}_{\nu(\bar{\nu})} &= \frac{(2\pi)^4}{s_i s_f} \int \prod_k [\frac{d\vec{p}_{i,k}}{(2\pi)^3}] \prod_l [\frac{d\vec{p}_{f,l}}{(2\pi)^3}] \delta^{(4)}(\sum_{l'} p_{f,l'} - \sum_{k'} p_{i,k'}) \\ &\times \omega_{\nu(\bar{\nu})} \sum_{i,f} | < f|H^{\alpha}_W|i > |^2 \; \Xi \; , \end{aligned} \tag{18}$$

where $\omega_{\nu(\bar{\nu})}$ is the energy of the emitted neutrino (anti-neutrino) and s_i and s_f are symmetry factor when two-nucleons in the initial or final state are identical particles. Ξ represents the occupation probability of incoming particles and the Pauli blocking of outgoing particles:

$$\Xi = \prod_{k=\text{initial particle}} f_k(p_k) \prod_{l=\text{final fermion} \neq \nu(\bar{\nu})} (1 - f_l(p_l)) \tag{19}$$

with

$$f_k(p_k) = \frac{1}{\exp((e_k(p_k) - \mu_k)/k_B T) \pm 1} \tag{20}$$

where one should use "+" ("−") for a fermion (boson); e_k (μ_k) is the energy (chemical potential) of the particle of the k-th kind, and $k_B T$ is the temperature multiplied by the Boltzmann constant. Note that the Pauli blocking factor for the final-state neutrino (anti-neutrino) is not included in Ξ. Explicit expressions for the cross sections and emissivities for the various processes under consideration are given in the Appendices.

4. Neutrino production cross sections

In this section we discuss the cross sections for neutrino emissions via DBF, (1)-(5), evaluated for initial kinetic energies up to ∼100 MeV. Fig. 1 shows the calculated cross

sections for e^-/e^+ capture on a deuteron, (1) and (2); the left panel is for $e^-+d \rightarrow n+n+\nu_e$, and the right panel is for $e^++d \rightarrow p+p+\bar{\nu}_e$. The cross sections for the two reactions are almost the same except in the very low-energy region, where the e^+-capture cross section is larger than the e^--capture cross sections due to Q-values differences. In the low-energy region, $E_e < 50$ MeV, the dominant transition is the Gamow-Teller transition to the $^1S_0$ scattering state, and the contribution of the MEC is less than 5%. It is noteworthy that, in the low-energy region, the cross section for e^- (e^+)-capture on the deuteron is smaller than that on the proton (neutron) by a factor larger than 3, mainly due to the higher threshold energy. In the higher energy region $E_e \sim 150$ MeV, the cross section for e^- (e^+)-capture on a bound proton is almost comparable to that on a free proton. The consequences of this feature in actual supernova environments will be discussed later in the text.

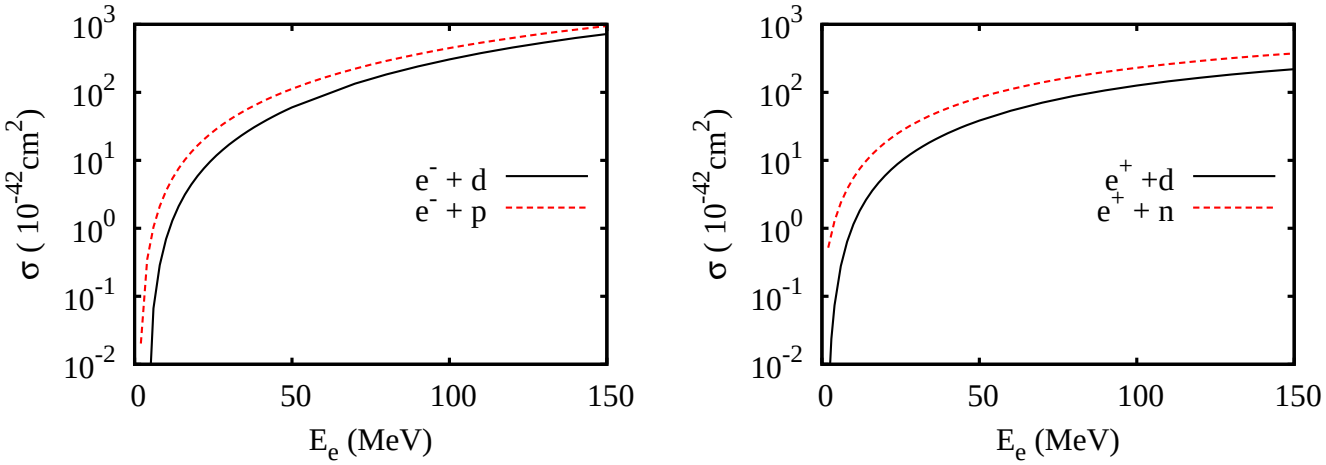

Fig. 1.— The cross sections for e^-/e^+-capture on the nucleon and the deuteron as functions of the e^-/e^+ energy E_e. The solid and dashed curves in the left (right) panel show the cross sections for electron (positron) capture on the deuteron and the proton (neutron), respectively.

Fig. 2 shows the cross sections for neutrino production in nucleon-nucleon collision

leading to the formation of a deuteron, reactions (3)-(5). The cross sections for the CC processes are about four times larger than the NC process, partly due to the isospin and the symmetry factors for the initial identical nucleons. Since the processes, (3) and (5), are exothermic reactions, their cross sections follow the $1/v$ law in the low-energy region. Although *pp*-fusion, (4), is also an exothermic reaction, it does not obey the $1/v$ law because Coulomb repulsion between the protons reduces the transition probability as v tends to zero. Our result for the *pp*-fusion cross section in the keV region agrees well with the previous work of Schiavilla et al. (1998). We remark that, to calculate the neutrino processes in a supernova environment, it is necessary to include two-nucleon partial waves up to $J_{NN} < 6$ (J_{NN}: total angular momentum) and to consider the two-nucleon relative kinetic energy, T_{NN}, up to $T_{NN} \sim 100MeV$. Effective field theory to describe such a kinematical region is just now becoming available (Baru et al. 2013). As T_{NN} increases, the importance of initial-state partial waves other than $^1S_0$ quickly increases, and furthermore, the contribution of MEC grows and becomes as important as the IA contribution. For $T_{NN} > 20$ MeV, the Gamow-Teller transition from the initial two nucleon $^1D_2$ state becomes a dominant transition amplitude. At the higher energies the most important MEC contribution comes from the Δ-excitation in the axial-vector current. It is the tensor character of this current which produces a large matrix element between the $^1D_2$ scattering state and the deuteron S-wave. It is notable that, even though the relevant supernova temperature is $T = 10 - 20$ MeV, the neutrino emissivity for $NN \to d$ at $T \sim 15$ MeV receives the largest contribution from the energy region $T_{NN} \sim 100$ MeV.

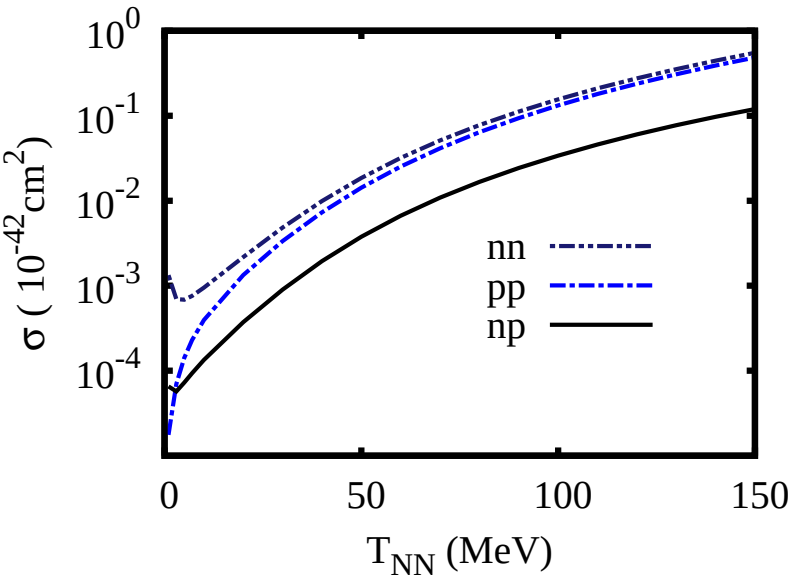

Fig. 2.— The cross sections for $p+n \to d+\bar{\nu}_x+\nu_x$(solid, black), $p+p \to d+e^+ +\nu_e$(dash-dot, blue) and $n+n \to d+e^- +\bar{\nu}_e$ (dash-two-dot, dark-blue) are plotted as a function of T_{NN}.

5. Neutrino emissivities

5.1. Supernova profiles

In order to study the consequences of neutrino emissions due to DBF for the supernova-explosion mechanism, we calculate neutrino emissivities for a given profile of a core-collapse supernovae, and compare the emissivities due to DBF with those arising from the conventional processes. To this end, we consider two representative profiles of a supernova core, Compositions I and II.

Composition I is the one obtained in (Sumiyoshi et al. 2005) in simulating gravitational collapse and core bounce for a 15 $M_\odot$ star ($M_\odot$: solar mass). This composition, which represents a typical situation of the post-bounce phase with a stalled shock wave, has

been obtained from a numerical simulation adopting the Shen equation of state (EOS) (Shen et al. 1998a,b, 2011). Composition I includes only nucleons, ^{4}He and a single heavy nucleus in the Shen EOS. Fig. 3 shows the temperature (T) and the density (ρ) as functions of the distance r from the supernova center, pertaining to a snapshot at 150 ms after the core bounce.

To assess the significance of the new additional emissivities due to DBF, we consider Composition II, which includes the mass fractions of the light elements obtained from the nuclear statistical equilibrium model (Sumiyoshi & Röpke 2008), i.e., nucleons, deuterons, tritons, ^{3}He, ^{4}He and other nuclei are taken into account. We remark that Compositions I and II share the same data for the profiles of ρ, T and Y_e. shown in Fig. 3. The nucleon chemical potentials needed to calculate the emissivities are also taken from the Shen EOS.

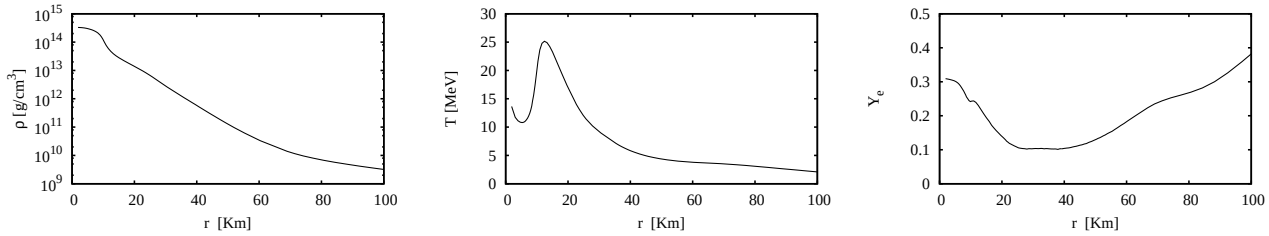

Fig. 3.— The density(left panel), temperature (middle panel) and electron fraction (right panel) distributions pertaining to a snapshot at 150 ms after the core bounce taken from (Sumiyoshi & Röpke 2008). The horizontal axis, r, is the distance from the supernova center.

Two regions in the profile will be discussed separately: the surface region of a proto-neutron star ($r > 20$ km, $\rho < 10^{13}$ g/cm^3) and the inner region ($r < 20$ km, $\rho > 10^{13}$ g/cm^3). The former corresponds to the neutrino-sphere region between the surface of the nascent proto-neutron star and the shock wave, where neutrino cooling and heating are

important. The latter corresponds to a high density region in the core of the proto-neutron star. One can legitimately question the existence of free-space deuterons in dense nuclear medium like the core region. Our aim here is to make a first study of possible influences of deuteron-like correlations that may persist even in the core region. Obviously our results for the core region obtained with the use of free-space deuterons are of exploratory nature and should be taken as such. The calculated emissivities are shown in Figs. 4-9.

5.2. Emissivity from the surface region of a proto-neutron star

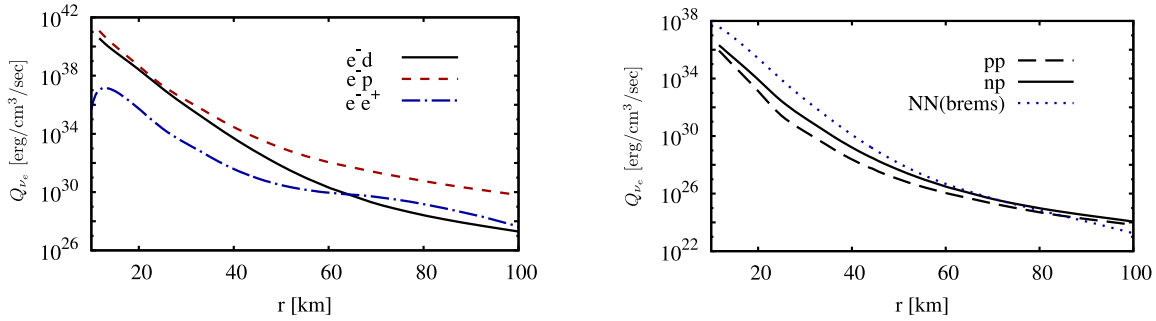

Fig. 4.— The ν_e-emissivities are shown as functions of the distance r from the center of the supernova evaluated with composition II except NN bremsstrahlung. In the left panel, the neutrino emissivities due to e^- captures on deuteron (1) and proton (6), and e^+e^- annihilation (11) are shown in solid, dashed and dash-dotted curves, respectively. In the right panel, the emisivities due to the pp and np fusion processes, (4) (5), and NN bremsstrahlung (10) are shown in long-dash, solid and dotted curves, respectively. The emissivities due to the reactions (10) and (11) are taken from Ref. Sumiyoshi et al. (2005).

To set the stage for examining the possible influences of ν_e-emissivities due to DBF, we first present ν_e-emissivities due to the conventional reactions calculated for Composition II except nucleon-nucleon bremsstrahlung (10), which is calculated for Composition I.

The left panel in Fig. 4 shows the emissivities arising from e^-p capture (6) and e^-e^+ annihilation (11), while the right panel gives the emissivities due to nucleon-nucleon bremsstrahlung (10). The figure indicates that e^-p capture gives a dominant contribution, and nucleon-nucleon bremsstrahlung (10) and the pair-production process (11) give only minor contributions to the emissivity.

The left panel in Fig. 4 also gives the neutrino emissivity due to e^--capture on the deuteron (1). The neutrino emissivity due to e^--capture on the deuteron is almost the same magnitude as that on the proton (6) around $r \approx 30$km. In this region, the mass fraction of deuteron is comparable or even larger than that of proton. We will discuss below the role of including the composition of light elements in the neutrino emissivity.

In Fig. 4 (right panel) it is shown that the neutrino emissivities from deuteron formation (4) and (5) are orders of magnitude smaller than those from e^--captures, (1) and (6), and the pair-production process (11). However, the neutrino emissivities from deuteron formations become comparable to the $\nu\bar{\nu}$ emissivity from nucleon-nucleon bremsstrahlung for distances closer to 100 km in the cooling region.

As for the $\bar{\nu}_e$-emissivity shown in Fig. 5, e^+-capture on the neutron (7) is dominant over the other processes due to the very large neutron abundance as well as the relatively large cross sections. As seen, the emissivity due to e^+-captures on the deuteron (2) is smaller than those on the neutron by a factor of 10^2–10^3, but is comparable to the pair-production process for $r < 40$ km. The emissions from nucleon-nucleon bremsstrahlung and deuteron formation are also smaller than e^+ capture on the deuteron. We observe that the deuteron formation from nn and np is comparable to that from NN bremsstrahlung and is significant in the outer region.

As we have seen in the previous section, the electron capture cross section of deuteron is smaller than that of proton. This indicates that the effective neutrino emissivity *per*

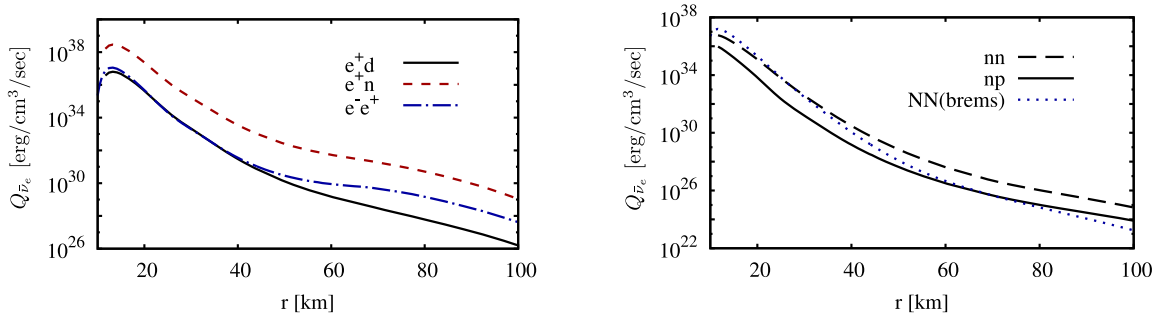

Fig. 5.— The $\bar{\nu}_e$-emissivities evaluated with Composition II except NN bremsstrahlung. In the left panel, the emissivities due to e^+ captures on a deuteron (2) and a neutron (7), and e^+e^- annihilation (11) are shown in solid, dotted and long dashed curves, respectively. In the right panel, the emissivities due to the nn (3) and np (5) fusion processes and NN bremsstrahlung(10) are plotted in dash-two-dotted, solid and two-dotted curves, respectively

proton via e^--captures on the proton is reduced if a substantial amount of protons in a supernova are bound in deuterons (and tritons). In fact, this is seen in Fig. 6. The left panel in Fig. 6 shows that the free proton abundance for Composition II(solid curve) is smaller than that for Composition I(short dashed curve) by a factor of $\sim$2, where deuteron(long dashed curve) is abundant. The total emissivity due to the e^--capture on protons in this region is effectively reduced by up to 40% as shown in the right panel in Fig. 6, where the solid curve shows ratio of the neutrino emissivity from e^--captures on the proton and deuteron for Composition II to that from e^--captures on the proton for Composition I. Meanwhile, as can be seen from the short dashed curve in the right panel of Fig. 6, the total anti-neutrino emissivity is only slightly affected by the deuteron abundance, mainly due to the dominant abundance of the neutron in the matter. The reduction of the total neutrino emissivity indicates that, in considering the neutrino emissivities due to electron-captures, it is important to take due account of the abundances of deuterons and other light elements.

Fig. 7 shows ν_μ-emissivities due to np fusion (deuteron formation), NN bremsstrahlung

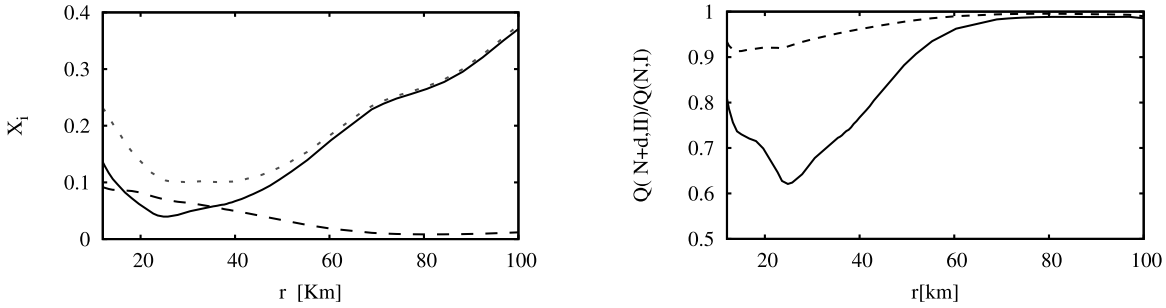

Fig. 6.— Left panel: Mass fraction of proton (solid curve) and deuteron (long dashed curve) for Composition II and that of proton(short dashed curve) for Composition I. Right panel:The ratio of the neutrino emissivity due to e^--capture(solid curve) and e^+-capture(short dashed curve) calculated for Composition II to that calculated for Composition I.

and e^+e^- annihilation. We note that the np fusion contribution is comparable to the NN bremsstrahlung contribution around $r = 60$ km, and the former becomes more important for $r \gtrsim 80$ km. In other words, emission of neutrino pairs through deuteron formation may contribute to additional cooling when NN bremsstrahlung is an important process.

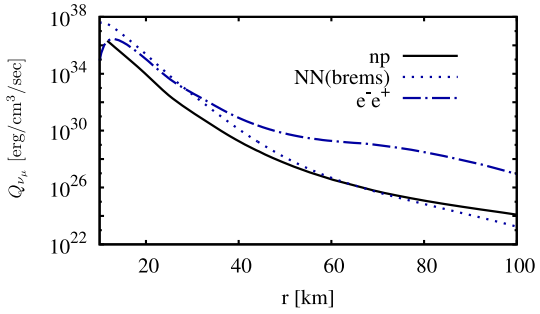

Fig. 7.— The ν_μ-emissivities evaluated with Composition II except NN bremsstrahlung. The contributions of np fusion, NN bremsstrahlung and e^+e^- annihilation are shown in solid, double-dotted and dashed lines, respectively.

5.3. Inner region of a proto-neutron star

In this high density region the deuteron is strongly modified and is not bound. As mentioned earlier, the "deuteron" used in our calculation should be regarded as a simplistic devise to simulate possible two-nucleon tensor correlation in nuclear matter. It is hoped that the results in this section give us some hint on whether we need to go beyond the mean-field nuclear matter approach and include possible two-nucleon correlations. With this caveat in mind we present the neutrino emissivities via the "deuteron" formation processes in the central part of the supernova core. Figs. 8 and 9 show the results obtained with the use of Composition I. The graphs in Figs. 8 and 9 indicate that neutrino emissions via "deuteron"

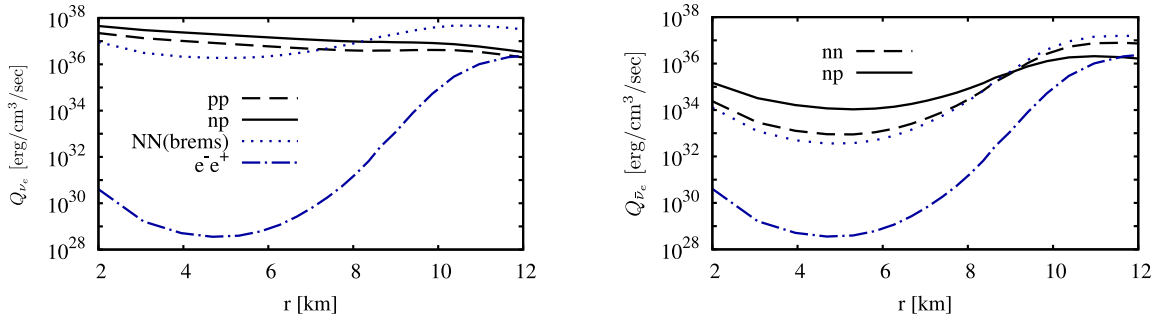

Fig. 8.— The ν_e-emissivities (left panel) and $\bar{\nu}_e$-emissivities (right panel) in the inner core region evaluated with Composition I. See captions for Figs. 4 and 5 for details.

formation become dominant for $\nu_e, \bar{\nu}_e$ and ν_μ. Since the electrons are highly degenerate in the core ($r < 10$ km), the pair process is strongly suppressed and nucleon-nucleon bremsstrahlung is a dominant channel in the conventional models. However, the figures show that neutrino pair emission from the neutron-proton weak fusion process (5) is much larger than those from the conventional processes, in particular for $\bar{\nu}_e$. The reaction (5) is favored by its positive Q-value due to the "deuteron" binding energy, and by the absence of Pauli-blocking in the final state. Hence, neutrino emission via "deuteron" formation from nucleon-nucleon scattering may play an important role in the neutrino pair production

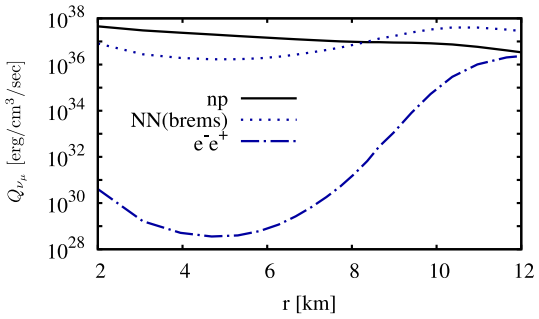

Fig. 9.— The ν_μ-emissivities in the inner core region calculated with Composition I. See the caption for Fig. 7 for details.

process and for the transport of heat and leptons inside proto-neutron stars. It is desirable to examine further the abundance of "deuteron" (n-p tensor correlations) in dense nuclear matter.

6. Discussion and summary

It was pointed out in Refs. Sumiyoshi & Röpke (2008) and Arcones et al. (2008) that, in addition to deuterons, tritons can also have large abundances in high density regions (10^{11}–10^{14} g/cm^3), where the electron fraction Y_e is low and the temperature T is high. This suggests the possible importance of neutrino emissivities involving the triton or "triton" (triton-like three-nucleon correlation in dense matter). In the present work, however, we have not considered these effects.

Our study here is based on the spherical (1D) configurations of supernovae. It would be interesting to study neutrino emission with the abundance of light elements in 2D/3D profiles. Hydrodynamical instabilities can generate non-spherical distribution of matter in the cooling region around a proto-neutron star and the heating region behind a stalled shock wave. Since the density, temperature and electron fractions can have wider ranges

in 2D/3D profiles, there may be regions of high deuteron abundance that cannot be found in the 1D profile. The existence of deuterons in the heating regions can contribute to the additional source of heating as studied by Nakamura et al. (2009). It thus seems interesting to study the possible effects of the neutrino emission and absorption channels involving the deuteron in multi-D supernova explosion simulations. In principle, one must study effects of all neutrino processes by solving the neutrino transfer and hydrodynamics, with detailed information on composition from the equation of state of supernova matter. A study along this line has been recently made (Furusawa et al. 2013a), taking into account the neutrino processes involving neutrino absorption on the deuteron and the light element abundance.

We now summarize. Neutrino emissions from $e^{\mp}$-capture on the deuteron and from deuteron formation in nucleon-nucleon weak-fusion processes have been studied as new neutrino emission mechanisms in supernovae. These weak processes are evaluated with the standard nuclear physics approach, which consists of the one-nucleon impulse current and two-nucleon exchange current and nuclear wave functions derived from high-precision phenomenological NN potentials. It is found that the contribution of the two-nucleon meson-exchange current is only a few % for the $e^{\mp}$-capture reactions, while it can be as large as the one-nucleon current contribution for the NN fusion reaction at higher energies. The consequences of these new neutrino-emission channels have been examined for representative profiles of core-collapse supernovae at 150 ms after core bounce. The emissivity due to the $e^{\mp}$ capture reaction on the deuteron is found to be smaller than that on the free nucleon. Therefore, as Fig. 6 indicates, the total neutrino emissivity due to electron capture on protons and deuterons is suppressed when an appreciable amount of protons in a supernova are bound inside deuterons. This results in a smaller neutrino luminosity and the lower efficiency of neutrino heating behind a stalled shock wave. Therefore, this new process may contribute unfavorably towards a successful supernova explosions. It might lead to a slower speed of the deleptonization and, hence, a slower evolution of nascent proto-neutron stars.

On the other hand, as seen in Figs. 4 and 5, neutrino emission via deuteron formation can be comparable to nucleon-nucleon bremsstrahlung in the outer region. This implies that there might exist situations in which the deuteron-formation weak processes are the main channels for neutrino emission.

In the inner core region, where the electrons are highly degenerate (high densities at low temperatures), pair-production via e^-e^+ annihilation is suppressed, making nucleon-nucleon bremsstrahlung a main channel to produce $\nu\bar{\nu}$ pairs among the conventional processes(Suzuki 1993; Burrows et al. 2006). Meanwhile, "deuteron" formation processes in NN scattering can have large rates for ν_μ and ν_τ emissions, a feature that may have significant consequences for the cooling of compact stars. Furthermore, the possible modification of the energy spectra of ν_e, ν_μ and ν_τ due to "deuteron" formation may influence supernova nucleosynthesis (Woosley et al. 1990; Yoshida et al. 2004) and the terrestrial observation of supernova neutrinos (Nakazato et al. 2013). On the other hand, the possible increase of the ν_μ and ν_τ fluxes due to "deuteron" formation hardly affects the heating process behind a shockwave, because these low-energy ν_μ and ν_τ interact with stellar matter only through the NC. As explained earlier, the "deuteron" here stands for a tensor-correlated NN pair that may persist even in dense nuclear matter. A detailed study of deuteron-like two-nucleon tensor correlation in dense matter seems well warranted, but it is beyond the scope of our present exploratory work.

This work was partially supported by JSPS KAKENHI Grant Numbers 25105010,20105004, 22540296, 24244036 and 24540273. K. Sumiyoshi is grateful to G. Röpke, S. Furusawa, S. Yamada and H. Suzuki for fruitful collaborations on the composition of light elements in dense matter and the numerical simulations of supernovae. K.S. acknowledges the usage of the supercomputers at Research Center for Nuclear Physics (RCNP) in Osaka University, The University of Tokyo, Yukawa Institute for Theoretical

Physics (YITP) in Kyoto University, and High Energy Accelerator Research Organization (KEK). SXN is a Yukawa Fellow and his work is supported in part by Yukawa Memorial Foundation. FM is supported in part by the National Science Foundation (US) Grant No. PHY-1068305.

A. Emissivity and cross section

A.1. Nuclear Matrix Elements

The matrix element $< f|H_W|i >$ is evaluated by using the multipole expansion formula given in Nakamura et al. (2001). The transition probability of electron(positron) capture $e^{\mp}(p) + i \to \nu(\bar{\nu})(p') + f$ for the initial two nucleon state $i(|LSJT, M >)$ and the final state $f(< L'S'J'T', M'|)$ is written as

$$\sum_{spin's} | < f(L'S'J'T', M'); \nu(\bar{\nu})(p')|H_W^{\alpha}|i(LSJT, M); e^{\mp}(p) > |^2 \;\; = \;\; 2(4\pi)X_{\alpha}^{\mp}(f, i; p', p). \tag{A1}$$

Here L, S, J and T are the orbital, spin, total angular momentum and isospin of the two-nucleon state. We sum over all spin components of the leptons and two-nucleon states. For α =CC and NC reactions, $X_{\alpha}^{\mp}$ is given as

$$\begin{aligned} X_{\alpha}^{\mp}(f, i; p', p) \;\; = \;\; & \frac{G_F^2}{2} F_Z(E) \begin{pmatrix} V_{ud}^2 \\ 1 \end{pmatrix} \sum_{J_o} [\\ & | < T_C^{J_o}(\mathcal{V}) > |^2 (1 + \vec{\beta} \cdot \vec{\beta}' + \frac{q_0^2}{\vec{q}^2} \, (1 - \vec{\beta} \cdot \vec{\beta}' + 2\hat{q} \cdot \vec{\beta} \hat{q} \cdot \vec{\beta}') - \frac{2q_0}{q} \, \hat{q} \cdot (\vec{\beta} + \vec{\beta}')) \\ & + | < T_C^{J_o}(\mathcal{A}) > |^2 (1 + \vec{\beta} \cdot \vec{\beta}') + | < T_L^{J_o}(\mathcal{A}) > |^2 (1 - \vec{\beta} \cdot \vec{\beta}' + 2\hat{q} \cdot \vec{\beta} \hat{q} \cdot \vec{\beta}') \\ & + 2Re[< T_C^{J_o}(\mathcal{A}) >< T_L^{J_o}(\mathcal{A}) >^*] \, \hat{q} \cdot (\vec{\beta} + \vec{\beta}') \\ & + [| < T_M^{J_o}(\mathcal{V}) > |^2 + | < T_E^{J_o}(\mathcal{V}) > |^2 + | < T_M^{J_o}(\mathcal{A}) > |^2 + | < T_E^{J_o}(\mathcal{A}) > |^2] \\ & \times (1 - \hat{q} \cdot \vec{\beta} \, \hat{q} \cdot \vec{\beta}') \end{aligned}$$

$$\mp 2Re[< T_M^{J_o}(\mathcal{V}) >< T_E^{J_o}(\mathcal{A}) >^* + < T_M^{J_o}(\mathcal{A}) >< T_E^{J_o}(\mathcal{V}) >^*]\ \hat{q}\cdot(\vec{\beta}-\vec{\beta}')]$$

. (A2)

Here $\vec{\beta}=\vec{p}/e(p)$ is the velocity of the lepton with $\vec{p}$ and $\vec{p}'$ being the momentum of the electron (positron) and neutrino, and the momentum transfer $q_\mu = p_\mu - p'_\mu$. $F_Z(E)$ is the Fermi function to take account of the Coulomb correction for the electron wave function. The nuclear reduced matrix element $< O >=< f||O||i >$ of the multipole operator O is defined in Eq. (60) of Nakamura et al. (2001), which includes all information of the nuclear current and nuclear wave functions. For e^--capture on the deuteron, the above formula should be understood as

$$< \mathcal{O} > \ = \ \sum_{L=0,2} < L'S'J'T'; NN||\mathcal{O}||L, S=1, J=1, T=0; d > \qquad \text{(A3)}$$

where $|LSJT; d >$ is the deuteron bound state and $|L'S'J'T'; NN >$ is the two nucleon scattering state.

A.2. Electron and positron capture on deuteron

The cross section formula for the electron/positron capture reaction $e^-(p_e) + d(P_d) \to \nu_e(p_\nu) + n(p'_1) + n(p'_2)$ / $e^+(p_e) + d(P_d) \to \bar{\nu}_e(p_\nu) + p(p'_1) + p(p'_2)$ is given as

$$\sigma_{e^\mp - cap} \ = \ \frac{m_N}{3\pi\beta}\int_0^{p_{\nu,max}} dp_\nu p_\nu^2 p'_{NN}\int_{-1}^{1} d\cos\theta_{e\nu}\sum_{L',S',J',T'} X_{CC}^{\mp}(NN(L'S'J'T'=1), d; p_\nu, p_e). \qquad \text{(A4)}$$

Here N denotes neutron/proton for the electron/positron capture reaction. We have introduced the relative momentum $\vec{p}'_{NN} = (\vec{p}'_1 - \vec{p}'_2)/2$ and the center-of-mass momentum $\vec{P}' = \vec{p}'_1 + \vec{p}'_2$ of the final two nucleons. As usual, $P_d^2/2m_d \sim P'^2/4m_N$, where we have neglected the difference between the center-of-mass energy of two nucleons and the deuteron, and we have used $p'^2_{NN}/m_N = e_e(p_e) + m_d - p_\nu - 2m_n$.

The neutrino emissivity $Q_{\nu_e/\bar{\nu}_e}$ for electron neutrino or anti-neutrino is given as

$$\begin{aligned} Q_{\nu_e/\bar{\nu}_e} &= \frac{m_N}{8\pi^6}\int_0^\infty dp_e \int_0^{p_{\nu,max}} dp_\nu p_\nu^3 p_e^2 p'_{NN} < \Xi >_{\nu_e/\bar{\nu}_e} \\ &\times \int_{-1}^{1} d\cos\theta_{e\nu} \sum_{S'L'J',T'=1} X^{\mp}_{CC}(NN(L'S'J'T'=1),d;p_e,p_\nu). \end{aligned} \tag{A5}$$

Here $< \Xi >_{\nu_e/\bar{\nu}_e}$ is given as

$$< \Xi >_{\nu_e/\bar{\nu}_e} = f_{e^{\mp}}(p_e)\int d\vec{P}_d f_d(\vec{P}_d)(1-f_N(\vec{P}_d/2+\vec{p}'_{NN}))(1-f_N(\vec{P}_d/2-\vec{p}'_{NN})). \tag{A6}$$

The exact formula for the emissivity involves 8-dimensional integration. A standard approximation is introduced in order to make the numerical integration manageable. We factorize the angular dependence in the matrix element and Ξ as follows

$$\int d\Omega_{p'_{NN}} | < f|H_W|i > |^2 \,\Xi \sim \int d\Omega_{p'_{NN}} | < f|H_W|i > |^2 \times \int \frac{d\Omega_{p'_{NN}}}{4\pi}\Xi. \tag{A7}$$

A.3. Neutrino emission in nucleon-nucleon scattering

The cross sections for neutrino emission in nucleon-nucleon scattering $N(p_1)+N(p_2) \rightarrow d(P_d)+l(p_l)+\bar{l}(p_{\bar{l}})$ are given as

$$\begin{aligned} \sigma_{NN-fusion} &= \frac{2\mu_{NN}}{\pi p_{NN}} f_\alpha \int_0^{p_{max}} dp_l p_l^2 p_{\bar{l}}^2 \\ &\times \int_{-1}^{1} d\cos\theta_{l\bar{l}} \sum_{LSJT} X^{+}_{\alpha}(d, NN(LSJT); p_{\bar{l}}, p_l) \end{aligned} \tag{A8}$$

where $\alpha = CC$ for reactions (3) and (4) and $\alpha = NC$ for reaction (5). We denote the lepton momentum by p_l and the anti-lepton momentum by $p_{\bar{l}}$; $\vec{q} = -\vec{p}_l - \vec{p}_{\bar{l}}$ is the momentum transfer. We approximate the energy conservation relation as $e_{\bar{l}}(p_{\bar{L}}) = m_{N_1} + m_{N_2} + {p_{NN}}^2/(2\mu_{NN}) - e_l(p) - m_d$, where p_{NN} is the two-nucleon relative momentum, and μ_{NN} is the reduced mass . The isospin factor f_α is $f_\alpha = 1$ and $1/2$ for the CC and NC reactions, respectively.

The emissivity is given as

$$Q_{\nu/\bar{\nu}} = \frac{1}{4\pi^6}\int_0^\infty dp_{NN}\int_0^{p_{l,max}} dp_l p_{NN}^2 p_l^2 p_{\bar{l}} e_{\bar{l}}(p_{\bar{l}}) p_\nu < \Xi >_{\nu/\bar{\nu}} \times \int_{-1}^{1} d\cos\theta_{e\nu} \sum_{SLJT} X_\alpha^+(d, NN(LSJT); p_{\bar{l}}, p_l) \quad \text{(A9)}$$

The neutrino energy p_ν is either p_l or $p_{\bar{l}}$ for the neutrino or anti-neutrino emissivity, and

$$< \Xi >_{\nu/\bar{\nu}} = F(p_l, p_{\bar{l}}) \int d\vec{P} f_N(\vec{P}/2 + \vec{p}_{NN}) f_N(\vec{P}/2 - \vec{p}_{NN}). \quad \text{(A10)}$$

F for the CC reactions, (3) and (4), is given as

$$F(p_l, p_{\bar{l}}) = 1 - f_e(p_l) \text{ for } (3) \quad \text{(A11)}$$

$$= 1 - f_e(p_{\bar{l}}) \text{ for } (4), \quad \text{(A12)}$$

while F for the NC reaction, (5), is given as

$$F(p_l, p_{\bar{l}}) = 1 - f_\nu(p_l) \text{ for } Q_{\bar{\nu}} \quad \text{(A13)}$$

$$= 1 - f_{\bar{\nu}}(p_{\bar{l}}) \text{ for } Q_\nu. \quad \text{(A14)}$$

REFERENCES

Ando, S. & Kubodera, K. 2006, Phys. Lett., B633, 253

Arcones, A., Martínez-Pinedo, G., O'Connor, E., Schwenk, A., Janka, H.-T., Horowitz, C. J., & Langanke, K. 2008, Phys. Rev., C78, 015806

Baru, V., Hanhardt, C., & Myhrer, F. 2013, arXiv:, 1310.3505

Beringer, J. et al. 2012, Phys. Rev., D86, 010001

Bethe, H. A. 1990, Rev. Mod. Phys., 62, 801

Burrows, A., Reddy, S., & Thompson, T. A. 2006, Nucl. Phys., A777, 356

Doi, M., Sato, T., Ohtsubo, H., & Morita, M. 1990, Nucl. Phys., A511, 507

Furusawa, S., Nagakura, H., Sumiyoshi, K., & Yamada, S. 2013a, Astrophys. J., 774, 78

Furusawa, S., Sumiyoshi, K., Yamada, S., & Suzuki, H. 2013b, Astrophys. J., 772, 95

Hempel, M., Fischer, T., Schaffener-Bielich, J., & Liebendörfer, M. 2012, Astrophys. J., 748, 70

Janka, H.-T., Langanke, K., Marek, A., Martínez-Pinedo, G., & Muller, B. 2007, Phys. Rep., 442, 38

Kotake, K., Sato, K., & Takahashi, K. 2006, Rev. Prog. Phys., 69, 971

Kubodera, K. & Park, T.-S. 2004, Annu. Rev. Nucl. Part. Sci., 54, 19

Lattimer, J. M. & Swesty, F. D. 1991, Nucl. Phys., A535, 331

Nakamura, S., Sato, T., Ando, S., Park, T.-S., Myhrer, F., Gudkov, V., & Kubodera, K. 2002, Nucl. Phys., A707, 561

Nakamura, S., Sato, T., Gudkov, V., & Kubodera, K. 2001, Phys. Rev., C63, 034617

Nakamura, S. X., Sumiyoshi, K., & Sato, T. 2009, Phys. Rev., C80, 035802

Nakazato, K., Sumiyoahi, K., Suzuki, H., Totani, T., Umeda, H., & Yamada, S. 2013, Astrophys. J. Suppl., 205, 2:1

Park, T. S., Marcucci, L. E., R. Schiavilla, M. V., Kievsky, A., Rosati, S., K. Kubodera, D.-P. M., & Rho, M. 2003, Phys. Rev., C67, 055206

Sato, T., Niwa, T., & Ohtsubo, T. 1995, in Proceedings of the IVth International Symposium on Weak and Electromagnetic Interaction in Nuclei, ed. H. Ejiri, T. Kishimoto, & T. Sato (World Scientific, Singapore), 488

Schiavilla, R., Stokes, V. G., Glockle, W., Kamada, H., Nogga, A., Carlson, J., & Machleidt, R. 1998, Phys. Rev., C58, 1263

Shen, H., Toki, H., Oyamatsu, K., & Sumiyoshi, K. 1998a, Nucl. Phys., A637, 435

—. 1998b, Prog. Thoer. Phys., 100, 1013

—. 2011, ApJS, 197, 20

Sumiyoshi, K. & Röpke, G. 2008, Phys. Rev., C77, 055804

Sumiyoshi, K., Yamada, S., Suzuki, H., Shen, H., Chiba, S., & Toki, H. 2005, Astrophys. J., 629, 922

Suzuki, H. 1993, in Proceedings of the International Symposium on Neutrino Astrophysics: Frontiers of Neutrino Astrophysics, ed. Y. Suzuki & K. Nakamura (Tokyo: Universal Academy Press Inc.), 219

Suzuki, H. 1994, in Physics and Astrophysics of Neutrinos, ed. M. Fukugita & A. Suzuki (Tokyo: Springer-Verlag), 763

Tamura, K., Niwa, T., Sato, T., & Ohtsubo, H. 1992, Nucl. Phys., A536, 536

Woosley, S. E., Hartmann, D. H., Hoffman, R. D., & Haxton, W. C. 1990, Astrophys. J., 356, 272

Yoshida, T., Terasawa, M., Kajino, T., & Sumiyoshi, K. 2004, Astrophys. J., 600, 204

This manuscript was prepared with the AAS LaTeX macros v5.2.